# Surface Chemistry and Spectroscopic Study of the Nonamyloid-Beta Component Segment of α-Synuclein (61-95)

**by**

**Olaluwoye Sunday Oladimeji**

A Thesis Submitted in Partial Fulfillment

of the Requirements for the Degree of

Master of Science in Chemistry

Middle Tennessee State University

2019

Thesis Committee:

Dr. Chengshan Wang, Major Professor

Dr. Keying Ding

Dr. Ngee Sing Chong

## ACKNOWLEDGEMENTS

I would like to use this opportunity to express my gratitude to my research advisor Dr. Chengshan Wang for his constant support and guidance in my thesis research. Also, I would like to specially thank my thesis committee Dr. Ngee Sing. Chong and Dr. Keying Ding for the time spent reviewing my thesis and giving me valuable suggestion on my work. I would like to thank Dr. Leblanc and Dr. Shanghao Li of the University of Miami for the use of CD JASCO J-810 spectrometer for the collection of the circular dichroism data and their collaboration.

I would like to specially thank the MTSU College of Basic and Applied Sciences and College of Graduate studies for sponsoring and hosting programs for students like myself to present and share our research. The MTSU chemistry department has been very supportive in aiding my career goals by providing supporting resources to carry out chemistry research. Also, the MTSU chemistry department has helped graduate students to develop their professional skills by sponsoring students for conferences, which is important for me to achieve my career goals in graduate school.

Also, I want to thank Jessie Weatherly for his assistance during instrument breakdown. I would like to thank my friends also for their time and support.

Finally, I want to thank my parents Mr. & Mrs. Olaluwoye, and my siblings for their wonderful support. I am particularly grateful to have a mentor, Dr. Chengshan Wang, who has taken meticulous effort to ensure that my career as a chemist is an exciting one.

## ABSTRACT

Parkinson's disease is a neurodegenerative disorder, characterized by a progressive loss of the dopaminergic neurons in the *substantia nigra* portion of the mid brain. The degenerating dopaminergic neurons develop a hallmark deposition of Lewy bodies comprising of mostly abundant of α-synuclein, which is a protein of 140 amino acid residues. The primary structure of α-synuclein is divided into three parts: N-terminal residues 1-60; the nonamyloid-beta component (NAC) which spans residues 61-95 and is responsible for the aggregation; and residues 96-140 which comprise the negatively charged C-terminus.[34] Though, there is an abundance of α-synuclein (~ 1 % among the total proteins) in the brain, α-synuclein accumulates in the presynaptic terminals where high concentration of amphiphilic structure such as liposomes and cell membrane. Previously, α-synuclein has been spread at the air-water interface which was used to mimic the amphiphilic nature in vivo. Both circular dichroism (CD) and FTIR showed that α-synuclein transforms from unstructured conformation in aqueous solution to α-helix at the interface.[23] Here, the NAC part of α-synuclein (i.e., α-synuclein (61-95)) was synthesized and purified. α-Synuclein (61-95) was shown to form a stable Langmuir monolayer at the air-water interface. The CD results, show that α-synuclein (61-95) transforms from unstructured conformation in aqueous solution to α-helix at the air-water interface. Also, surface FTIR techniques have shown a parallel orientation of the helical axis of α-synuclein (61-95) to the interface.

## TABLE OF CONTENTS

## LIST OF FIGURES

## LIST OF TABLES

## LIST OF SCHEMES

# CHAPTER I

# INTRODUCTION

## 1.1 Parkinson's disease

Parkinson's disease (PD) is the second most common neurodegenerative disorder affecting over 1% of the people above the age of 65 years in the United States.[1] PD belongs to a category of conditions known as motor system disorders, which is due to the consequence of the loss of brain cells producing dopamine.[2] Because dopamine is a neurotransmitter responsible for communicating messages that plan and control body movement, the loss of dopamine causes the PD's symptoms such as bradykinesia, tremors, and postural instability (problems with walking or standing).[1,2] PD patients may develop difficulty in talking, walking, or completing other tasks when these symptoms become more pronounced.[2] Studies have revealed a number of pathological features in the PD-afflicted brain. Presently, there is no cure and available treatments offer only symptomatic relief to PD patients. The precise cause of Parkinson's disease is unknown, but the degenerating dopaminergic neurons develop an important hallmark deposition of Lewy bodies, which are related to a form of pathological proteinaceous aggregation in the brain. The primary protein component of the Lewy body is α-synuclein, which is found as amyloid fibrils in the aggregates.[3,7,8]

## 1.2 α-Synuclein

α-Synuclein is a 140-amino acid presynaptic protein, and the functions of α-synuclein are still poorly known.[7,9] It is a soluble, heat-resistant, acidic protein with an extended structure primarily composed of random coils. α-Synuclein consists of three domains: N-terminus domain, hydrophobic domain, and C-terminus domain. The sequence of α-synuclein ( see Scheme 1) shows: 1) the N-terminus domain (1-60 amino acids) which has positively charged lysine residue

and contains four 11-amino acids which imperfectly repeat; 2) the hydrophobic domain (61-95 amino acids), which is the central part of the protein and is known as the nonamyloid-beta component (NAC); 3) the C-terminus negatively charged domain (96-140 amino acids), which is rich in acidic residues and is responsible for the disordered structure of the protein, is the last part. NAC is related to Parkinson's disease because it is critical for the aggregation of α-synuclein.

α-Synuclein is a presynaptic neuronal protein linked genetically to PD, because its aberrant soluble oligomeric conformations (also known as protofibrils) are toxic in nature and are responsible for the disruption of cellular homeostasis. A hypothesis states that the natively unstructured α-synuclein molecules misfold to form various aggregates in the cytoplasm of the dopaminergic cells under adverse conditions, and it is explained below.[10,11]

MDVFMKGLSK AKEGVVAAAE KTKQGVAEAA GKTKEGVLYV GSKTKEGVVH GVATVAEKTK EQVTNVGGAV VTGVTAVAQK TVEGAGSIAA ATGFV*KKDQL GKNEEGAPQE GILEDMPVDP DNEAYEMPSE EGYQDYEPEA*

Scheme 1. The sequence of α-synuclein with the N-terminus underlined and the C-terminus in italics.

### 1.3 Conformation change of α-synuclein

Several interactions occur that give the protein certain structures. Protein structure is the arrangement of atoms in an amino acid-chain molecule in three-dimensions.[13] Two levels of protein structure are primary and secondary structures. The primary protein structure is the sequence of amino acids in the polypeptide chain (is a chain of monomers of amino acid). The secondary protein structure is the local conformation on the actual polypeptide backbone chain.[13] It is characterized by the intra- and intermolecular hydrogen bonds among the amino acid residues. The major typical secondary structures (also known as conformations) are β-sheets, α-helix, and random coils as shown in Figure 1. Random coil structure is also known as unstructured conformation.[13]

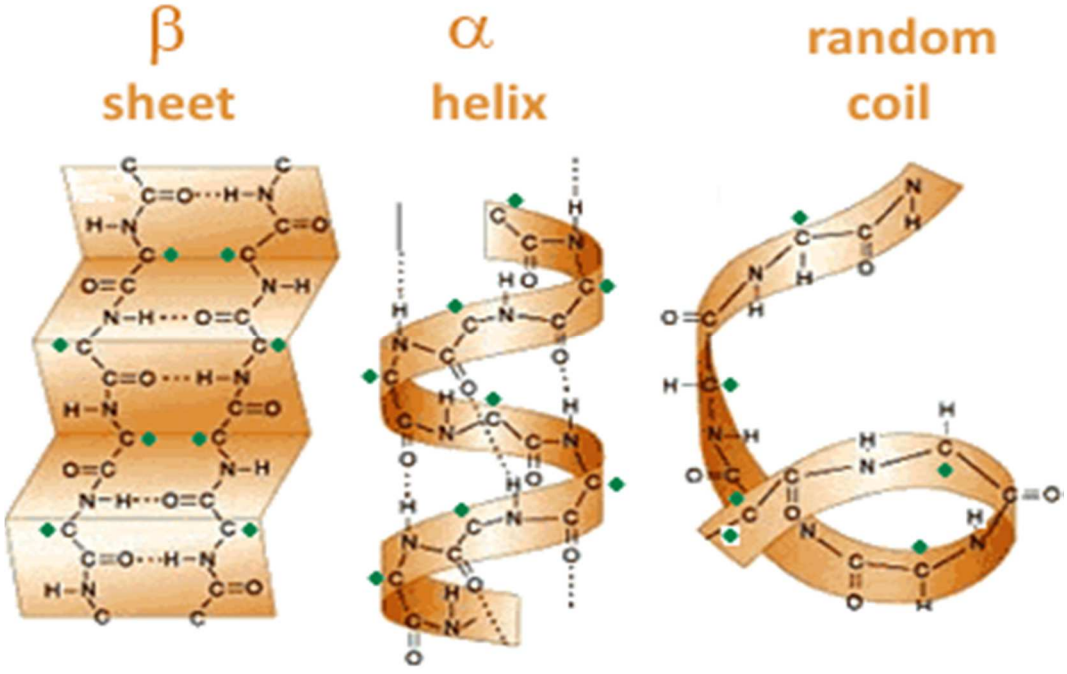


Figure 1. Secondary structure (orientation in space of chains of amino acids), adapted from reference[14].

While the native α-synuclein structure is unstructured, that does not mean it is an opened structure.[9] The natively unstructured protein can switch into various conformations depending on the environment and the binding.[9] Changes in the environment from the protein can lead to an increase of its hydrophobicity and/or decrease of its net charge, both of which induce partial folding. The NAC region gives α-synuclein the ability to also switch into a β-sheet conformation (Figure 2), which is identical to those detected in the Lewy bodies. Therefore, the aggregation procedure of α-synuclein has been widely studied in aqueous solution. The NAC-region shown in Scheme 1 is the most relevant region for PD because of its ability to oligomerize into fibrils.

α-Helical structure is induced when α-synuclein binds with lipids such as phospholipids.[9,10,12] α-Synuclein is found to be enriched near the presynaptic terminals (PST) of neurons where an abundance of vesicles exists.[11,17] Thus, among the different factors impacting the misfolding and aggregation of α-synuclein, phospholipid bilayers (e.g. cell membranes and vesicles) have attracted huge attention. However, the structure of lipid bilayers is complicated and is discussed below.

**1.4 Three regions of the structure of lipid bilayers**

The structure of phospholipid bilayers (see Figure 2) can be categorized into three parts:[18] 1) the hydrophilic head groups of the phospholipid bilayer; 2) the interior core of the membrane, which has the hydrophobic tail; 3) the lipid-water interfacial layer (LWIL) at which the dielectric constant is much smaller than the bulk water.[20,21]

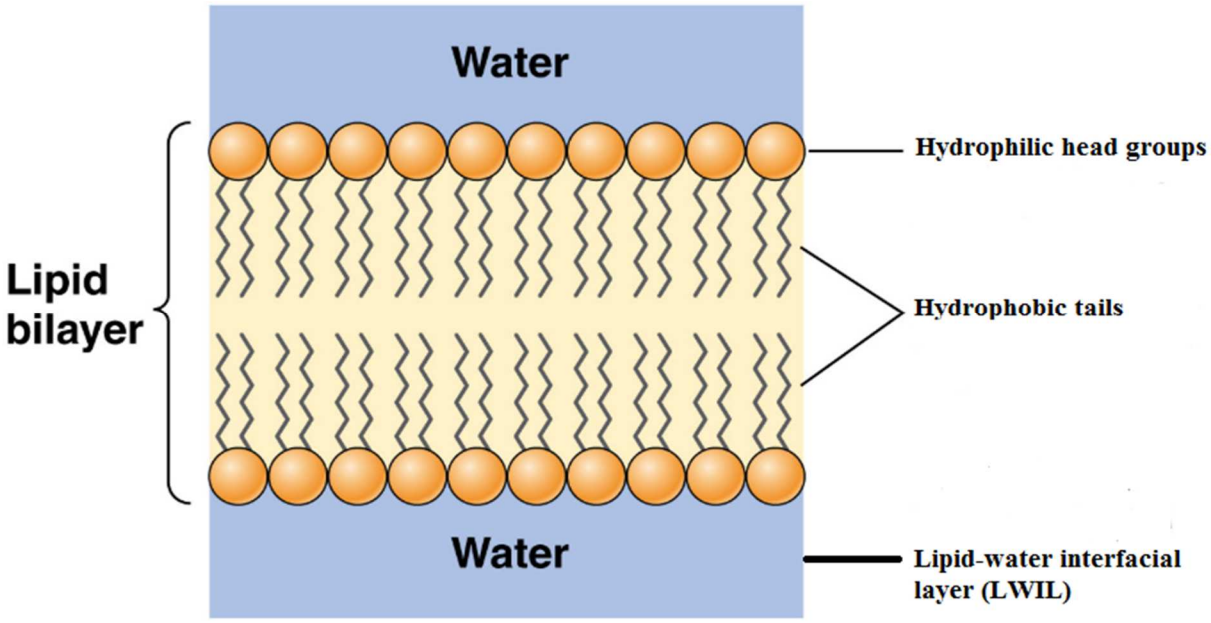


Figure 2. Basic structure of lipid bilayer, adapted from reference[19].

These three parts stay together and thus, it is challenging to determine which layer induces conformation change of α-synuclein. The air-water interface is simple, and it is well accepted as mimicry of the LWIL due to the similar dielectric constant between them.[22] The Langmuir monolayer technique is an accurate procedure to determine the chemical and physical properties (such as stability or aggregation) of the accumulation and interaction of protein molecules at the air-water interface. The Langmuir monolayer technique, as shown below, can be easily used to monitor physical parameters such as distance between molecules and surface pressure, which describes the interaction between molecules.

## 1.5 Techniques for protein structure determination

### 1.5.1 Langmuir monolayer technique

Langmuir monolayer is only one layer of amphiphilic molecules formed at the air-water interface. A Langmuir-Blodgett trough is an instrument used to measure the Langmuir monolayer, and it is diagramed in Figure 3. A Langmuir-Blodgett trough includes two barriers used to compress the Langmuir monolayer. The trough is rectangular, and the top holds the liquid phase where monolayers are fabricated. The trough top is often made of hydrophobic material (polytetrafluoroethylene) that improves sub-phase containment. Molecules, which may form a Langmuir monolayer, are deposited on the surface with a syringe.[24] The two shorter sides of the rectangular surface may be mechanically compressed by means of a movable barrier. Because both the available surface area and amount of substance deposited on the surface are known, the distance between the molecules at the surface can be used to describe area per molecule (or molecular area). A pressure sensor/electrobalance arrangement measures the surface pressure, and the area per molecule is obtained from the total area given by the barrier position. As the molecular area decreases, the molecules will be compressed together. This compression results into molecular interactions, which increase the surface pressure of the interface to which the molecules are confined. The surface pressure decreases the surface tension of the liquid due to the presence of the monolayer. The surface pressure-area ($\pi$-A) isotherm obtained by compressing the monolayer is the most commonly used character in the description of a monolayer. The increase in surface pressure is detected by an inert probe, which contacts, but does not significantly penetrate, the air-water interface. This is accomplished by decreasing the tension it exerts on the mass balance from which it hangs. Spectroscopic methods can be combined with the Langmuir monolayer technique to elucidate the structure of the monolayer.

Specifically, multiple-angle incidence resolution spectroscopy (MAIRS) which is a Fourier transform infrared spectroscopy (FTIR) technique is one of the most important spectroscopic methods that can be used. The FTIR Spectroscopy of protein/peptide and MAIRS are explained in Section 1.5.2 and 1.5.3, respectively.

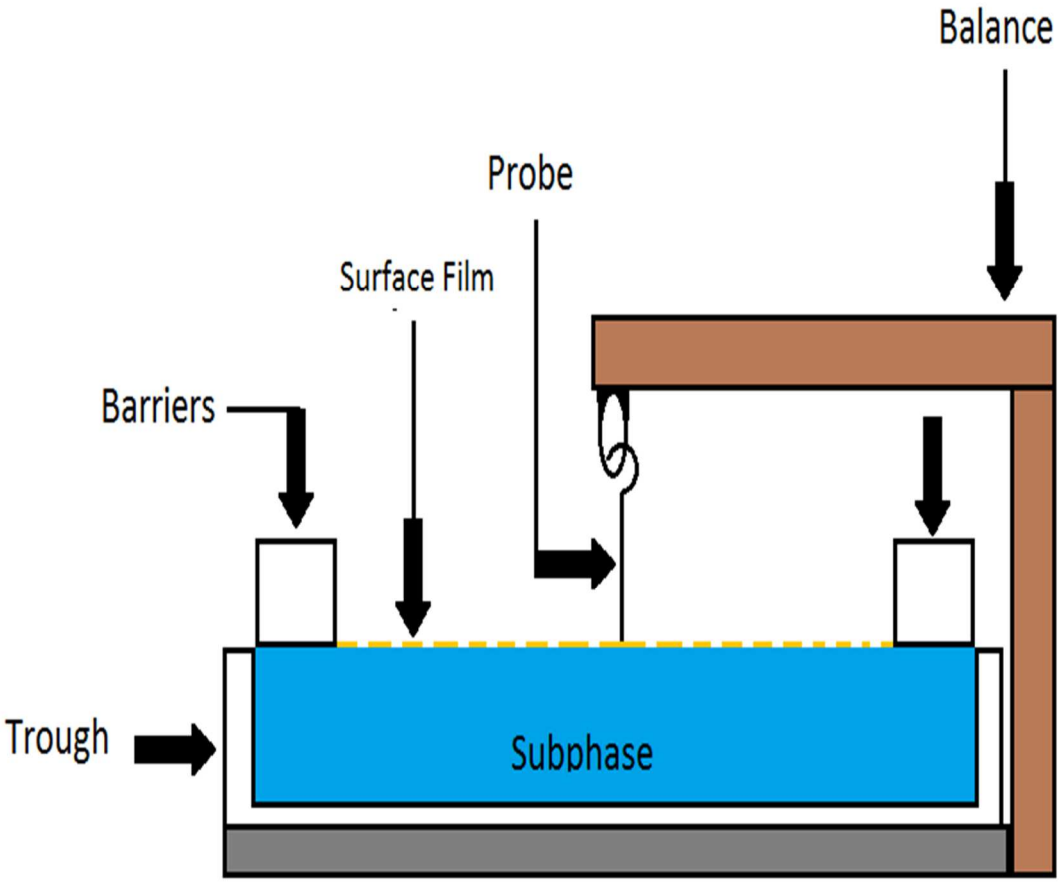


Figure 3. Langmuir trough diagram, reprinted with permission from reference[32].

### 1.5.2 Amide bands of proteins in FTIR

FTIR is one of the few techniques that is used for the analysis of structural characterization of peptides and proteins in different environments. The amide functional group of the polypeptide backbone absorbs infrared radiation, giving rise to nine characteristic 'amide' IR bands shown in Table 1. These 'amide' IR bands are A, B, and I through VII.[20,24-26] Some of these vibration modes are shown in Figure 4.

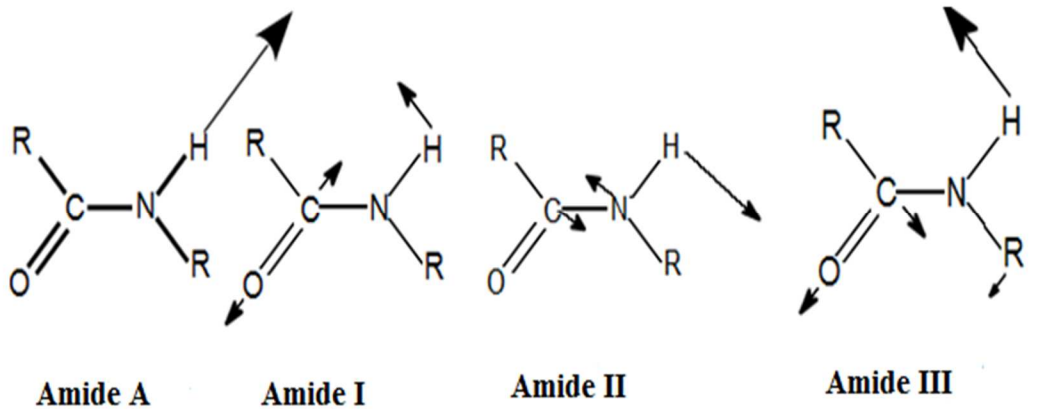


Figure 4. Peptides bond vibration modes, reprinted from reference[27].

Specifically, the Amide I band absorption ranges from 1600-1700 $cm^{-1}$. The C=O stretching vibrations of the amide carbonyl contribute about 85% to this band, and the position of the amide I band is related to the secondary structure of proteins and peptides as shown in Table 2.[23] Unstructured conformation, for instance, shows a peak at ~1640 $cm^{-1}$ for the Amide I band, and the peak of β-sheet is ~1630 $cm^{-1}$. The peak position is significantly affected by the helix of

α-helical segments. For a long helix, the peak will appear at ~ 1648 $cm^{-1}$ and shifts to a higher frequency as the helix becomes shorter.[23,26]

Table 1: Characteristic infrared bands of peptide linkage

| Designation | Approximate Wavenumber ($cm^{-1}$) | Description |
|---|---|---|
| Amide A | 3300 | NH stretching |
| Amide B | 3100 | NH stretching |
| Amide I | 1600-1690 | C-O stretching |
| Amide II | 1480-1575 | CN stretching, NH bending |
| Amide III | 1229-1301 | CN stretching, NH bending |
| Amide IV | 625-767 | OCN bending |
| Amide V | 640-800 | Out-of-plane, NH bending |
| Amide VI | 537-606 | Out-of-plane, C-O bending |
| Amide VII | 200 | Skeletal torsion |

Table 2: Characteristic Amide I frequencies of protein secondary structure

| Wavenumber ($cm^{-1}$) | Assignment |
|---|---|
| 1690-1680 | β sheet structure |
| 1666-1659 | α-helix (short) |
| 1657-1648 | α-helix (long) |
| 1645-1640 | Random coil |
| 1630-1620 | β sheet structure |

Except for the amide IR bands mentioned above, amide bands are composed of overlapping frequencies of the vibrations of multiple functional groups but are not often used for secondary structural studies. Furthermore, Multiple-angle incidence resolution spectroscopy (MAIRS) has also been used to study the orientation of proteins/peptides that forms Langmuir-Blodgett (LB) film and it is explained below.

### 1.5.3 Multiple-angle incidence resolution spectroscopy

MAIRS of protein monolayer films at the interface provides unique molecular structure and orientation information from the film constituents. This technique is thus well-suited for studies of protein interaction in a physiologically relevant environment. MAIRS is a useful spectroscopic tool for uncovering the molecular anisotropic structure in a thin film. In addition, MAIRS is used for the molecular orientation investigation of many functionalized organic thin films.[28] This spectroscopic technique gives both in-plane (IP) and out-of-plane (OP) vibration mode spectra, as shown in Figure 5. Both IP and OP are determined by the angles of incidence selected, which also reveals the molecular orientation. MAIRS shows the surface-parallel ($x$) and surface-perpendicular ($z$) components of a transition moment, respectively, from an identical sample. Since both $x$ and $z$ components are available for every absorption band, MAIRS makes the molecular orientation analysis of each chemical group an easy task irrespective of the degree of crystallinity of the thin film.[28] Due to the ability of the MAIRS spectra for revealing molecular orientation, at the interface of a Langmuir-Blodgett (LB) film, it is a good choice for studying protein monolayers. In addition to FTIR, CD is another technique used to analyze the structure of peptides/proteins.

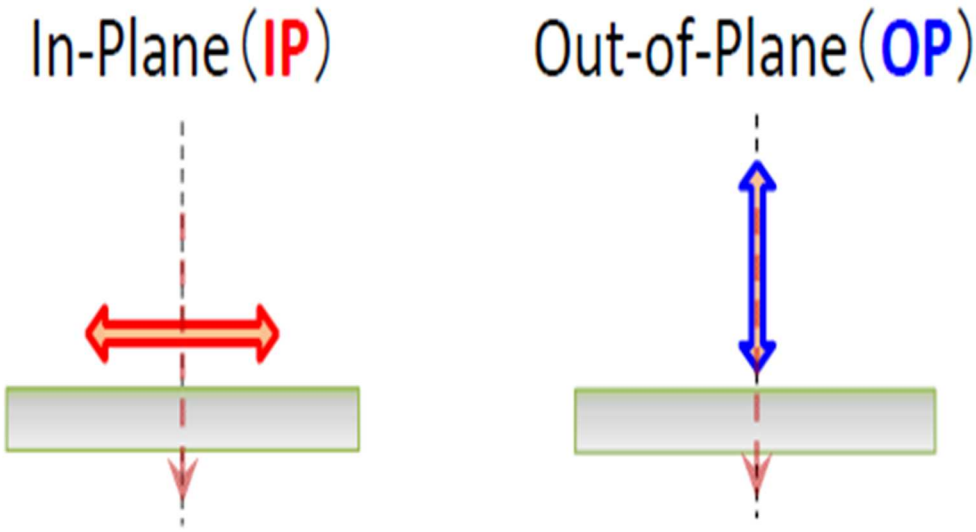


Figure 5. In-plane and Out-of-plane vibration modes, reprinted from reference[28].

### 1.5.4 Circular dichroism spectroscopy

CD studies of proteins and peptides have been carried out in the biophysical and biochemical sciences.[10,24,26,30] CD utilizes circular polarized light to monitor structural changes of proteins. It's sensitivity to protein conformation makes the measurement of CD achievable within several minutes. Proteins usually show strong CD signals between 260 nm and 180 nm due to the large amount of carbonyl groups (C=O which absorbs intensively around 200 nm) in the backbone of amide bonds.[24,29] Due to carbonyl arrangement in different conformations (such as β-sheet, α-helix, and unstructured conformation), every secondary structure shows its distinct patterns in the CD spectrum.[10,29]

The far-UV CD β-sheet conformation exhibits a positive peak at 196 nm and a negative peak at 215 nm. The α-helix conformation shows two characteristic negative peaks at 222 nm and 208 nm and one positive peak at 192 nm. Only one negative peak at 199 nm will be detected

in the unstructured conformation as shown in Figure 6.[10,29] Conformation and orientation of peptides at the interface have been explained in detail by surface chemistry techniques such as the Langmuir monolayer technique together with FTIR and CD. These surface chemistry spectroscopic techniques provide helpful information for biochemistry and biophysics. Surface chemistry and surface spectroscopy study of α-synuclein is a good example.

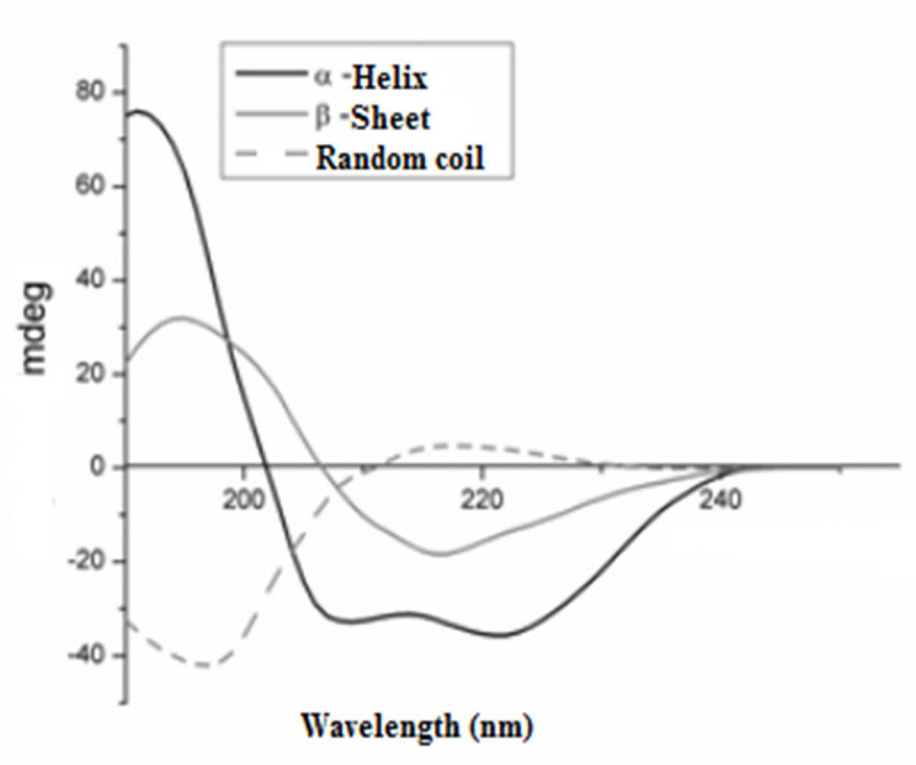


Figure 6. CD spectra of protein secondary structural elements, adapted from reference[31].

### 1.6 Surface chemistry and surface spectroscopy study of α-synuclein

α-Synuclein has been shown to form a Langmuir monolayer at the air-water interface, and the monolayer was found to be stable.[24] As previously stated in Section 1.2, that α-synuclein in

aqueous solution is in an unstructured conformation which has never been reported to form a stable Langmuir monolayer. Thus, it is very interesting to study the conformation of α-synuclein at the air-water interface. α-Helix is characterized by two negative peaks at 222 nm and 208 nm with one positive peak at 192 nm. These peaks were observed when the CD spectrum of quartz slides was deposited with α-synuclein Langmuir monolayer. This is an indication that α-synuclein is in α-helix rather than unstructured conformation at the air-water interface. For further confirmation, the surface FTIR spectra of α-synuclein detected the Amide I band at 1655 $cm^{-1}$, which is assigned to α-helix. Therefore, by combining the results of Langmuir monolayer technique, CD, and FTIR, it can be concluded that the unstructured α-synuclein in aqueous solution transforms to α-helix when spread at the air-water interface. [24]

## 1.7 Thesis proposal

There is still no consensus concerning the interaction of amphiphilic nature with the NAC part, which is the key for the pathology of PD. Previously in our group, the NAC part (i.e., α-synuclein (61-95)) has been synthesized by Fmoc (fluorenylmethyloxycarbonylchloride) solid phase synthesis and purified by high performance liquid chromatography (HPLC).[32] The NAC part (i.e., α-synuclein (61-95)) has been spread on the air-water interface and was found to form Langmuir monolayer.

In this study, a Langmuir monolayer technique will be used to detect stability of the Langmuir monolayer of the α-synuclein (61-95) at the air-water interface. Since α-synuclein is known to be in an unstructured conformation in pure water.[23] The Langmuir monolayer of the α-synuclein (61-95) will be transferred on to a quartz slide by Langmuir monolayer technique.

This will then be examined in an aqueous solution for possible conformational change from an unstructured conformation to α-helix at the air-water interface by circular dichroism. Furthermore, the Langmuir monolayer of α-synuclein (61-95) will also be transferred on to a silicon slide by a Langmuir monolayer technique in an aqueous solution and the molecular orientation of Langmuir monolayer of the α-synuclein (61-95) at the air-water interface will be investigated by MAIRS.

# CHAPTER II

# MATERIALS AND METHODS

## 2.1 Materials

Table 3: Lists of materials used in this thesis and their respective suppliers.

| Materials | Purity % | Supplier |
|---|---|---|
| Piperidine | 99.00 | Sigma-Aldrich (St. Louis MO) |
| Fmoc-Asparagine | 99.69 | Novabiochem (Hohenbrunn, Germany) |
| Fmoc-Aspartic acid | 99.69 | Novabiochem (Hohenbrunn, Germany) |
| Fmoc-Glutamine | 99.61 | Novabiochem (Hohenbrunn, Germany) |
| Fmoc-Glutamic acid | 99.11 | Novabiochem (Hohenbrunn, Germany) |
| Fmoc-Glycine | 99.37 | Novabiochem (Hohenbrunn, Germany) |
| Fmoc-Isoleucine | >98.00 | Novabiochem (Hohenbrunn, Germany) |
| Fmoc-Leucine | 99.80 | Novabiochem (Hohenbrunn, Germany) |
| Fmoc-Phenylalanine | >98.00 | Novabiochem (Hohenbrunn, Germany) |
| Fmoc-Serine | 99.83 | Novabiochem (Hohenbrunn, Germany) |
| Fmoc-Threonine | 99.60 | Novabiochem (Hohenbrunn, Germany) |
| Fmoc-Valine | 99.53 | Novabiochem (Hohenbrunn, Germany) |
| HOBT (hydroxybenzoyltriazole) | >99.00 | Anaspec Inc. (Fremont, CA) |
| Wang Resin | >99.00 | Novabiochem (Hohenbrunn, Germany) |
| DCM (Dichloromethane) | 99.60 | Fisher Scientific (Fairlawn, NJ) |
| Acetonitrile | 99.90 | Fisher Scientific (Fairlawn, NJ) |

| | | |
|---|---|---|
| DMF (N,N-dimethylformamide) | 99.80 | Fisher Scientific (Fairlawn, NJ) |
| Diethyl ether | 99.90 | Fisher Scientific (Fairlawn, NJ) |
| DMAP (4-dimethylaminopyridine) | ≥ 99.00 | Fisher Scientific (Fairlawn, NJ) |
| Tris (Triisopropysilane) | 98.00 | Sigma-Aldrich (St. Louis, MO) |
| Nitrogen gas | 99.99 | Airgas (Radnor, PA) |
| DIC (Diisopropylcarbodiimide) | 99.00 | Anaspec Inc. (Fremont, CA) |

**2.2 Peptide Synthesis**

Solid Phase Peptide Synthesis was used to synthesize the peptides in this thesis using CEM peptide synthesizer. Peptides are grown on an insoluble polymer which is a solid support and the vital step in the solid-phase synthesis is the selection of the solid support. The solid support used in this thesis was Wang resin, which has a labile of p-hydroxybenzyl alcohol linker joined to the top of a polystyrene bead. The Wang resin is used because it has the following properties: good swelling, mechanical strength and it support easy cleavage of peptides in moderate acidic conditions. The protection strategy used is known as fluorenylmethyloxycarbonylchloride (Fmoc) chemistry. In this strategy, Fmoc was used to protect the amino group of the amino acids, which also prevents solution coupling of dissolved amino acids. Base-stable protecting groups are used to protect free amino acid side chains such as t-butyl for phenol on the tyrosine side chain, and tert-butoxycarbanyl protected amino side chains on lysine.

The target peptide is synthesized artificially from C-terminus to N-terminus by repeated cycles in the following order: Coupling-washing-deprotection-washing as shown in Figure 7-9. In the coupling step, the target peptide is synthesized from C-terminus to the N-terminus which allows the amine group of the free amino acid in the DMF solution to be protected by Fmoc group. The coupling of the first amino acid involves the coupling of the C-terminal of the amino acid to the Wang resin. DMAP is then used to catalytically accelerate the activation of the amino acid carboxyl with 0.2 molar equivalents of Wang resin. And then HOBt is added to suppress racemization followed by the addition of DIC to activate the carboxylic group. The activated carboxylic group reacts with the amine group on the surface of the solid phase to form an amide bond and the remaining free Fmoc-protected amino acid in the DMF solution is then released after the coupling. DMF is then used to wash the resin and to clean the surface of the solid phase.

In the deprotection step, a solution of 1: 4 by volume of piperidine to DMF mixture is used to initiate the deprotection step in the reaction vessel. The Fmoc group which protects the amine group reacts and link up with piperidine. As a result, the amine group will be deprotected and ready for the coupling of the next amino acid. And then, DMF is used to wash the resin and clean the surface of the solid phase.

Coupling and deprotection steps were repeated using the Fmoc protected amino acid present in the primary structure of the target peptide (see Schemes 1). When the peptide chain is complete, the peptide was removed from the resin by washing with DCM. And then, the resin was suspended in a 20 mL solution, in the volume ratios of 75: 22: 1.5: 1.5 volumes of TFA, DCM, triisopropylsilane and $H_2O$, respectively. Furthermore, the suspension was agitated to break the bond between the peptides C-terminal carboxylic group and the resin. $H_2O$ and

triisopropylsilane were utilized to scavenge both the t-butyl and tert-butoxycarbanyl protecting groups cleaved by the acid.

DCM is used to wash the synthesis vessel after cleaving the peptide, and the wash which includes DCM, TFA, triisopropylsilane and water are then removed via purging with nitrogen gas, then the peptide is precipitated in ethyl ether. The peptide is then pelleted from the ether using mild centrifugation in a 15 mL polypropylene tube. The resulting pellet was dried under vacuum to obtain the crude synthetic peptide. Small amount of the crude product is then dissolved in a mixture of DMSO and a drop of TFA which was then analyzed by Mass spectrometry (MS) and is explained below.

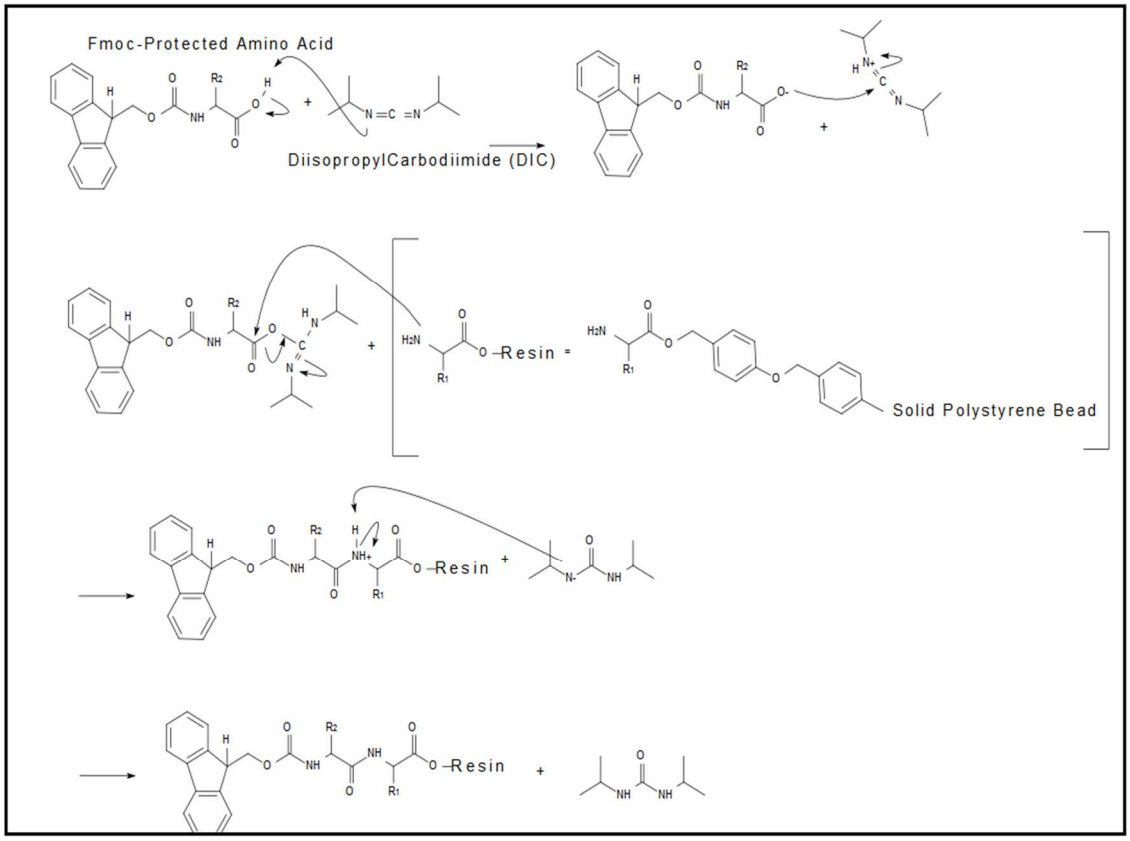


Figure 7. Coupling reaction in a peptide synthesis.

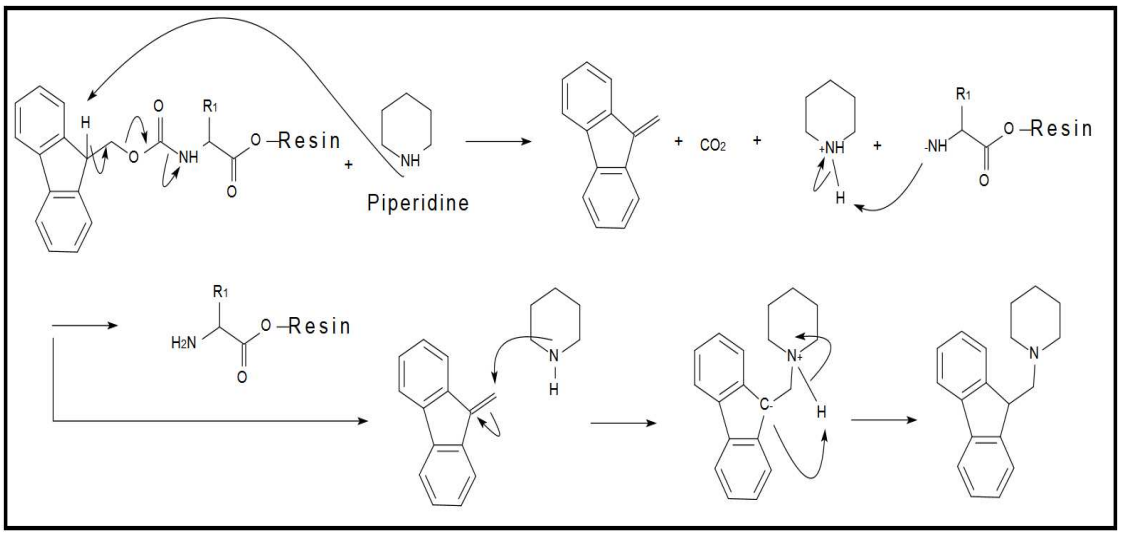


Figure 8. Deprotection reaction in a peptide synthesis.

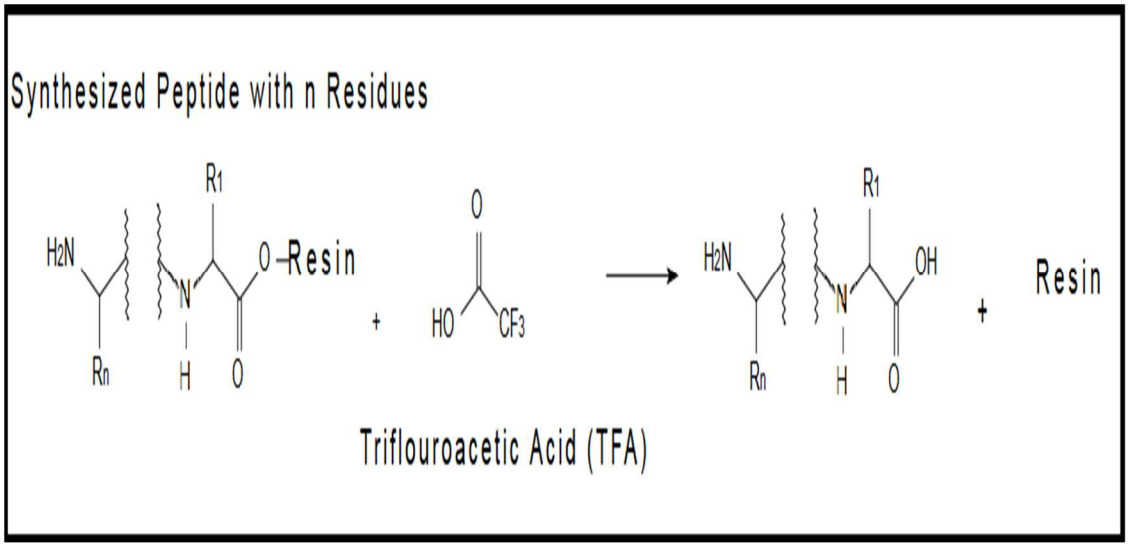


Figure 9. Cleavage reaction in a peptide synthesis.

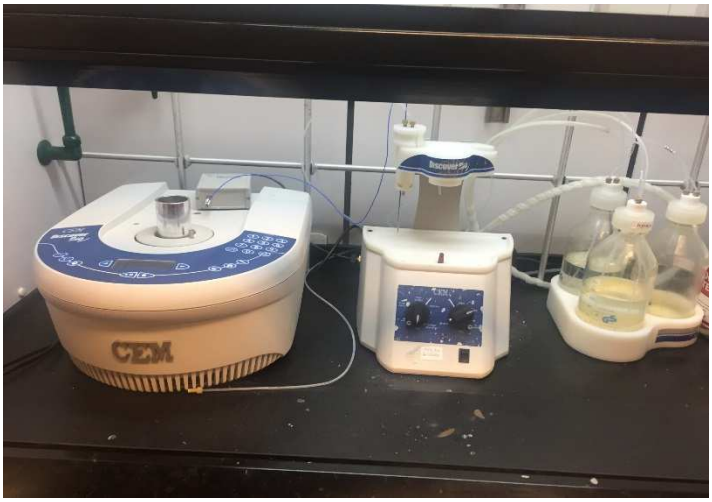


Figure 10. CEM peptide synthesizer instrument.

**2.3 Mass Spectrometry**

MS provides measurement of the molecular weight (MW) distribution of the compounds in a sample by ionizing chemical compounds to generate molecular fragment ions or molecular ions for measurement based on their mass to charge ratios. A mass spectrometer consists of three major components: ion source, mass analyzer, and a detector. The ion source converts the sample into ions; the extraction system transfers the ions from the sample into the mass analyzer. The mass analyzer separates the ions of various molecules by their mass-to-charge ratios and then passes the ions to the detector. The detector measures the signal intensities used for calculating the abundances of each ion present in the molecules.

Figure 11 shows a Waters Synapt model of a mass spectrometer (Milford, MA), with an Electrospray (ES)-Time of flight (TOF). This instrument was used for all the mass spectrometric measurements carried out in this thesis. The mass spectrometric measurements were done by nebulizing the liquid sample from a small capillary to create an aerosol which is ionized by a

Coulombic charge on the capillary. The ionized molecules are accelerated towards the detector with the help of an electric field gradient. As the ions are moving towards the detector, a mass analyzer separates them based on their mass to charge ratio. In this research, Time of Flight (ToF) mass analyzer is used, which utilized a magnetic field to separate the mobile ions. This separation allows the analysis of the MW of the ions. Crude product of α-synuclein (61-95) was dissolved in dimethylsulfoxide (DMSO) with 0.5 % TFA and injected into the MS. The MS capillary ionization voltage was set to 3.00 keV with a positive ion mode, at a temperature of 100 ºC and $N_2$ gas was used for desolvation and kept at a flow rate of 500 L/hour. The crude product was purified by high performance liquid chromatography (HPLC) as explained below.

Figure 11. Waters synapt tandem mass spectrometer with time-of-flight configuration.

**2.4 High performance liquid chromatography**

HPLC separates compounds on the bases of their affinity to the functionality of the surface of porous material packed into a chromatographic column. The affinities of the compounds are influenced by controlling the identity and concentration of the solvents used to dissolve the analyte. HPLC purification was carried out by using a solid support stationary phase known as column, which contains unmodified silica resins. When the material used in HPLC technique is functionalized with hydrophilic functionality, the technique is known as "normal phase chromatography". In normal phase chromatography, hydrophilic stationary phase is used. The mobile phase used as dissolved hydrophilic molecules in it because of the strong affinity of the stationary phase. As a result, the column tends to bind or adsorb the hydrophilic molecules in the mobile phase, though the hydrophobic molecules pass through the column and are eluted. When the material is functionalized with a hydrophobic functionality, the technique is known as reverse phase HPLC.

HPLC purification was performed on a Waters 1525 Binary Solvent Pump (Waters Corp., Milford, MA) shown in Figure 12 is attached to a Phenomenex Reverse Phase Semi Prep C18 Column, Jupiter Model 00G-4055- P0 with column dimensions of internal diameter of 21.5 mm and length of 250 mm (Phenomenex, Inc. Torrence, CA). The UV absorption detection wavelength was achieved by monitoring UV absorbance at 250 nm and was measured by a Waters 2489 UV-Vis detector (Waters Corp., Milford, MA). The separation of the α-synuclein (61-95) from impurities in the crude product was achieved by a ratio of a linear gradient of 8-16% by volume of A and B at a flow rate of 21.5 mL/minute for 50 minutes using water to 0.1% TFA by volume as mobile phase A, and acetonitrile to 0.1% TFA by volume as mobile phase B. The α-synuclein (61-95) retention time was identified by both MS and

fractionation. When the MW of the α-synuclein (61-95) was confirmed in the fraction, purification process was repeated for the rest of the crude products. The purified fractions collected were then frozen at -80 ° C and lyophilized to obtain the solid purified α-synuclein (61-95).

Figure 12: HPLC Waters 1525 system.

## 2.5 Circular Dichroism Spectroscopy

CD spectra in this thesis were measured by a JASCO J-810 spectropolarimeter attached with a 150-W xenon lamp as shown in Figure 13. The spectra were recorded with a response time of 4s and scan speed of 20 $nm \cdot min^{-1}$ for 2 complete scans.

Figure 13: CD Jason 810 spectrometer.

## 2.6 Multiple-Angle Incidence Resolution Spectroscopy

MAIRS was carried out on a Thermo Fischer Scientific Nicolet 6700 iS50R FTIR equipped with Thermo Fischer Scientific (Waltham, MA, USA) automatic MAIRS equipment XA-511 external reflection accessory with a mercury–cadmium–telluride detector shown in Figure 14, and cooled by liquid nitrogen. MAIRS was performed on a film of 35 µl 1.5 mg/mL α-synuclein (61-95) Langmuir monolayer on pure water subphase compressed to a surface pressure of 6 mN/m on a Kibron µ-trough S (Kibron Inc., Helsinki, Finland) Langmuir Trough.

MAIRS spectra were collected with 128 scans and 4 $cm^{-1}$ resolution. The IP and OP results were calculated by the p-MAIRS software.

Figure 14: Thermo Fischer Nicolet iS50R FTIR and electronic rotary stage.

**2.7 Langmuir trough**

A Kibron µtrough Langmuir trough XS (Kibron Inc., Helsinki Finland) was used for the acquisition and study of the stability of the surface pressure-area (π-A) isotherms and Langmuir monolayer of α-synuclein (61-95) on pure water subphase under the constant conditions of 20$^{o}$ C and 50 % relative humidity, respectively. α-Synuclein (61-95) aqueous solution of 1.5 mg/mL and 35 µL α-synuclein (61-95) was spread on air-water interface by a 25 µL syringe (Hamilton Inc., Reno, Nevada) held less than 1 cm from the subphase surface. α-Synuclein (61-95) Langmuir monolayers was held for 15 minutes before being transferred onto quartz slides under the surface pressure of 6 mN/m has Langmuir-Blodgett films of α-synuclein (61-95). The quartz slide was moved slowly at 0.3 cm/minute.

# CHAPTER 3

# RESULTS

## 3.1 Electrospray mass spectrum of α-synuclein (61-95)

The electrospray mass spectrum of α-synuclein (61-95) is shown in Figure 15. The peak noticeable at 1630.97 Da is designated to the diprotonated α-synuclein (61-95). The other two peaks at 1087.5 Da and 815.4 Da are as a result of the triple and quadruple protonated α-synuclein (61-95) respectively. The measured experimental molecular weight of α-synuclein (61-95) is 3261.9 Da from the peaks above, which is in proximity to the theoretical value at 3260.6 Da. There is no other peak detected, therefore the synthesis of α-synuclein (61-95) is successful. And then, the surface pressure-area (π－A) isotherm was studied to investigate the stability of the Langmuir monolayer of α-synuclein (61-95) and it is explained below.

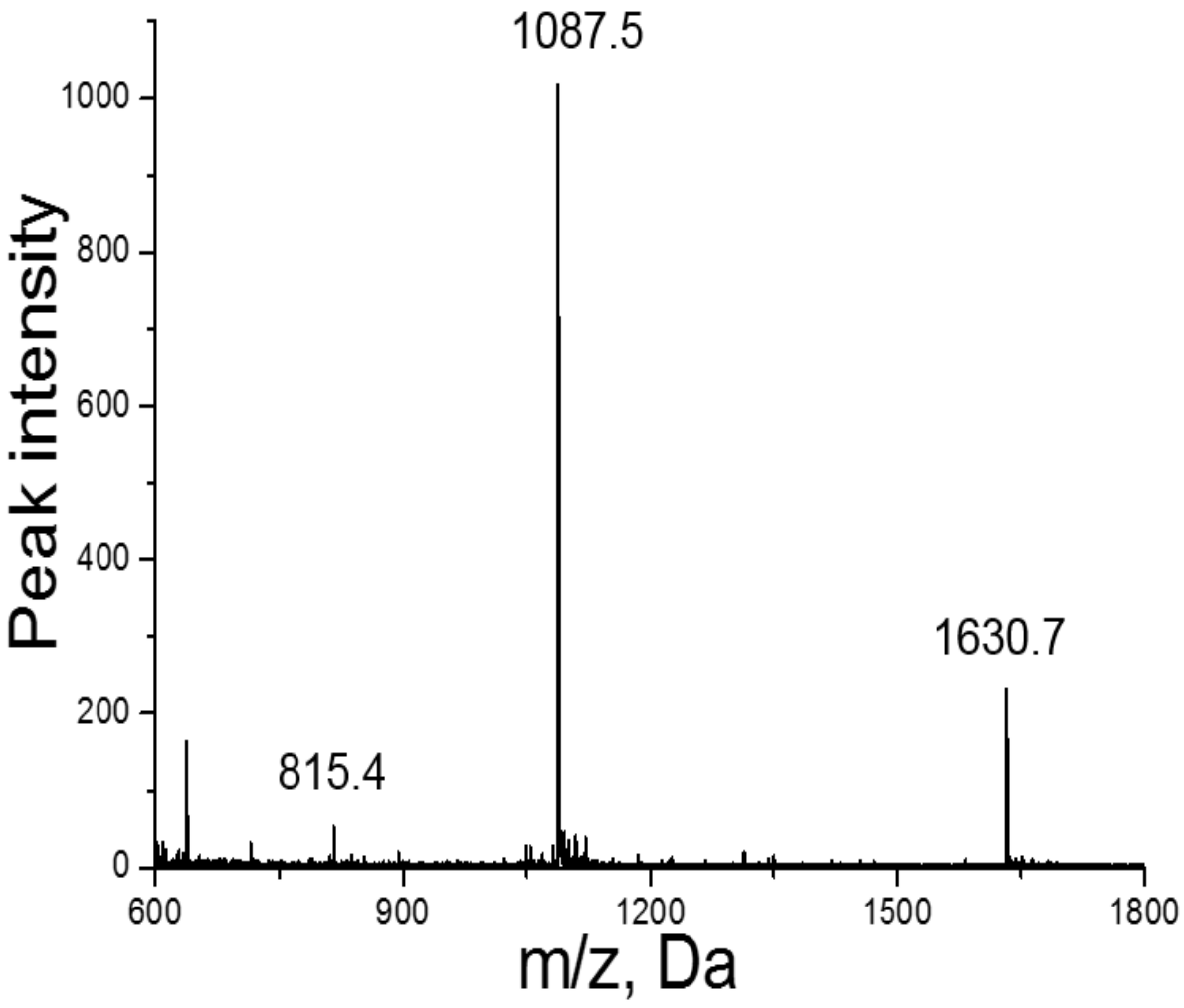


Figure 15. Mass spectrum of α-synuclein (61-95) reproduced with permission from reference[32]

### 3.2 Surface pressure area isotherm of α-synuclein (61-95)

Figure 16 shows the surface pressure-area (π－A) isotherm of α-synuclein (61-95). The take-of point of the π－A isotherm was at 400 $Å^2$/molecule when the subphase was pure water, and then a stable increase of the surface pressure up to twist point at 360 $Å^2$/molecule. When the surface area is lowered, this caused quick increase in the surface pressure and a fall was observed at surface pressure 17 mN/m with 205 $Å^2$/molecule. When the higher surface pressures of the isotherm is extrapolated to zero surface pressure, the limiting molecular area was acquired at 350 $Å^2$/molecule. In addition, there was a little increase in limiting molecular area when concentration of NaCl added into the subphase is 0.5 M.

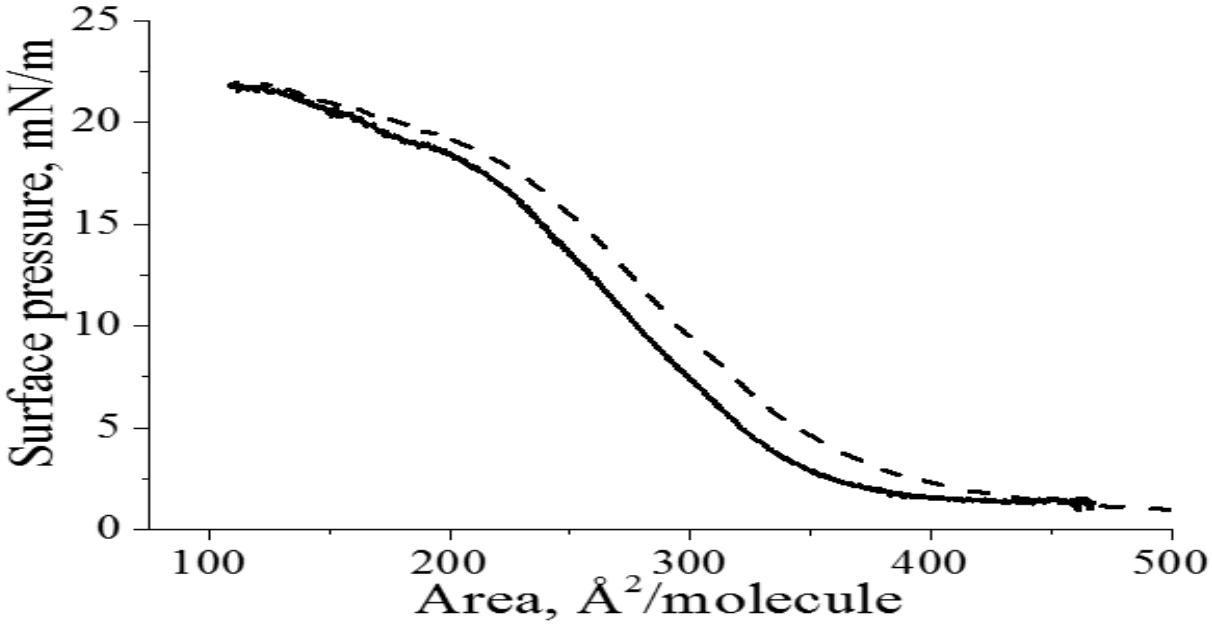


Figure 16. Surface pressure-area isotherm of α-synuclein (61-95) on: pure water (solid line) and 0.5 M NaCl (dashed line) subphase. Reprinted with permission from reference [33].

### 3.3 Stability study of Langmuir monolayer of α-synuclein (61-95)

Figure 17 shows that the Langmuir monolayer of α-synuclein (61-95) is stable. The α-synuclein (61-95) Langmuir monolayer was compressed to a surface pressure of 6 mN/m and the surface pressure is kept constant for over 120 minutes. The surface pressure and area are represented with solid line curve and dashed line curve respectively. These curves were monitored through-out this experiment as shown in Figure 17. When the α-synuclein (61-95) Langmuir monolayer was compressed to a target pressure of 6 mN/m, a decrease in area was observed. This decrease in area is almost identical to that in the surface pressure-area (π－A) isotherm at a pressure of 6 mN/m as shown in Figure 16. The space lost between the peptide molcules caused a little decrease in the molecular area for the first 30 minutes. Then also, the molecular area only lowered slightly unvaryingly after the 120 minutes of compression. Thus, signifies that Langmuir monolayer of α-synuclein (61-95) is highly stable. In addition, Langmuir monolayer of α-synuclein (61-95) was studied for possibility of denaturing in the first 30 minutes and it is discussed below.

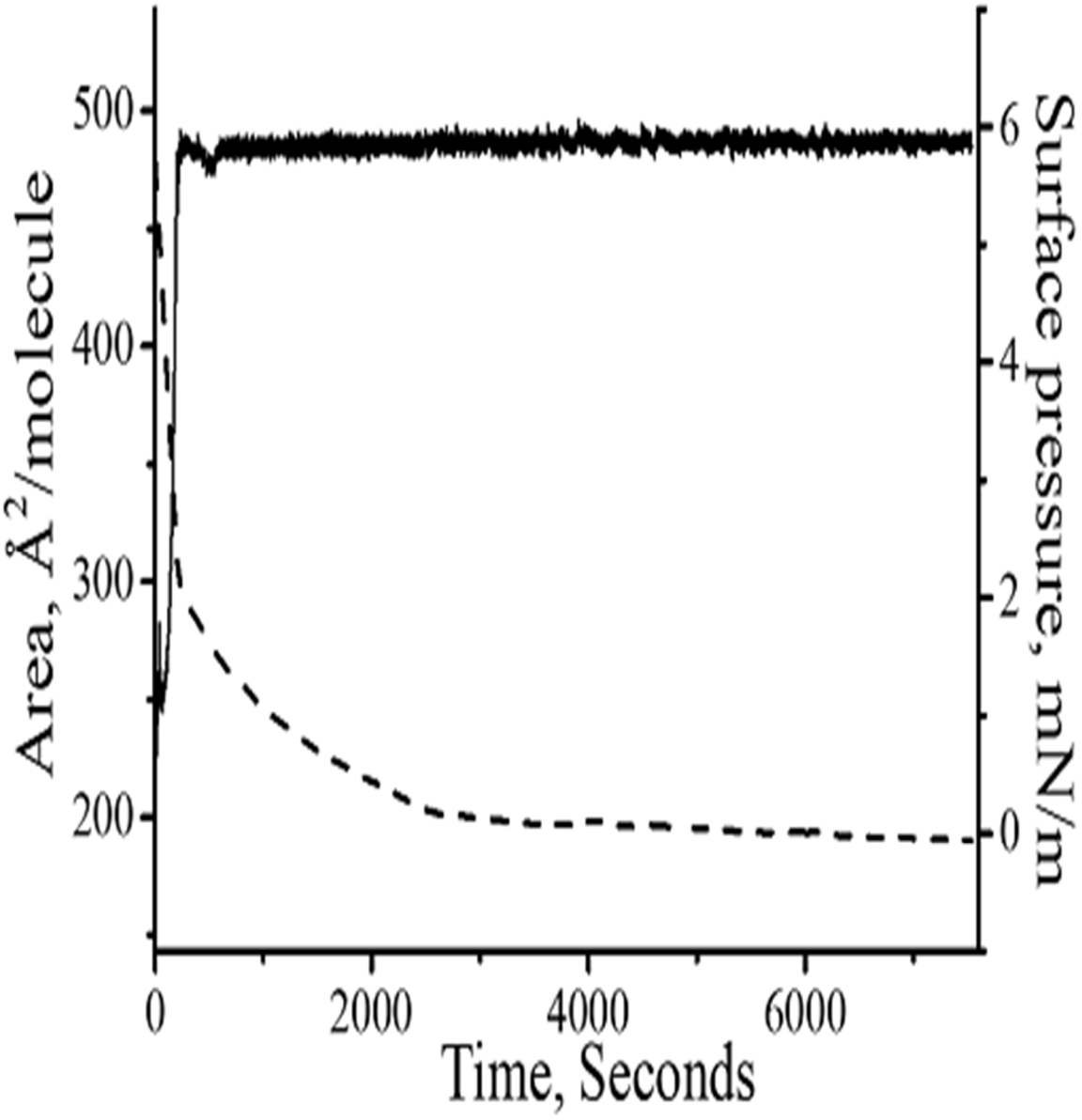


Figure 17: Stability curves when the Langmuir monolayer of α-synuclein (61-95) was compressed to a target pressure of 6 mN/m and kept constant for more than 120 minutes on pure water subphase. Surface pressure (solid curve) and molecular area (dashed curve).

### 3.4 CD spectrum of α-synuclein (61-95) Langmuir-Blodgett film

Langmuir monolayer of α-synuclein (61-95) is investigated for the possibility of denaturing in the first 30 minutes by transfering Langmuir monolayer of α-synuclein (61-95) onto quartz slides as Langmuir-Blodgett (LB) films. The CD spectra of both 0.075 mg/mL α-synuclein (61-95) dissolved in pure water and α-synuclein(61-95) LB film on quartz slide are dash line and solid line respectively as shown in Figure 18. The peak at 199 nm is the only negative peak detected when α-synuclein (61-95) is dissolved in aqueous solution, which was designated to unstructured conformation. For the LB films of α-synuclein (61-95) on quartz slides, three peaks were detected. Two negative peaks at 208 and 221 nm and one positive peak at 191 nm. The three peaks above are characteristic peaks of α-helix. There is no change in CD after holding the surface pressure for 2 hours. Thus, α-synuclein (61-95) transformed to α-helix in the LB film. Furthermore, the molecular orientation of the α-synuclein (61-95) was investigated by MAIRS and it is explained below.

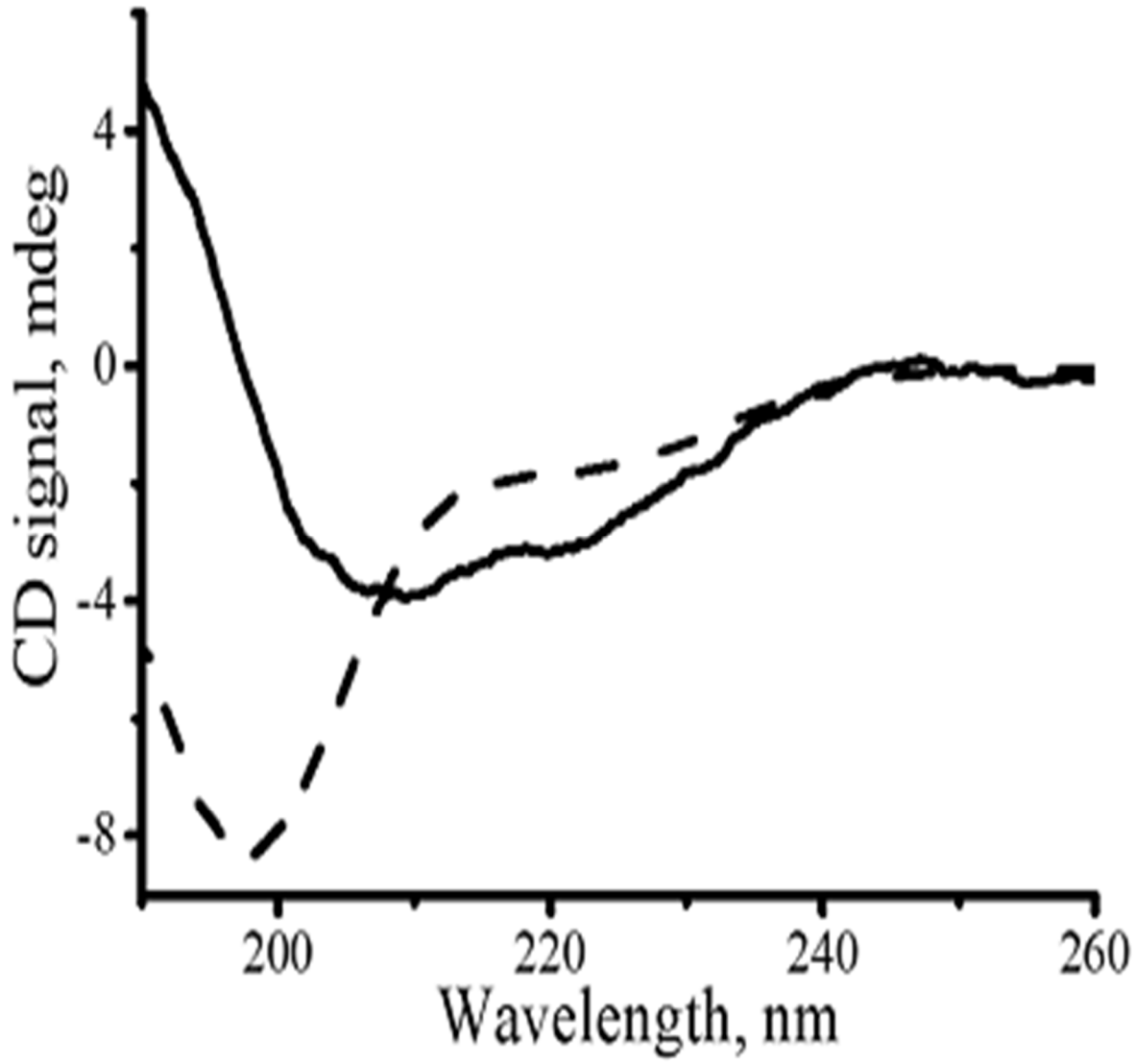


Figure 18: CD spectra of 0.075 mg/mL α-synuclein (61-95) dissolved in pure water (dash curve) and α-synuclein (61-95) LB film on quartz slide (solid curve). Reproduced with permission from reference [33].

### 3.5 MAIRS spectrum of α-synuclein (61-95) Langmuir-Blodgett film

Figure 19 shows that the molecular orientation of α-synuclein (61-95) LB film is surface-parallel to the air-water surface. The IP and OP spectra were calculated from the measured spectra at incident angle in the range of 1700 – 1600 $cm^{-1}$. In addition, due to hydration, the amide I is centered at 1658 $cm^{-1}$, meaning that α-synuclein (61-95) is in α-helix conformation, which is consistent with the CD result in Figure 18. Also, the amide I band is from C=O. However, the C=O stretching vibration band at 1658 $cm^{-1}$ clearly appears in the IP spectrum only, but is silent in the OP spectrum. This strongly suggests that the C=O group is oriented roughly parallel to the air-water surface.

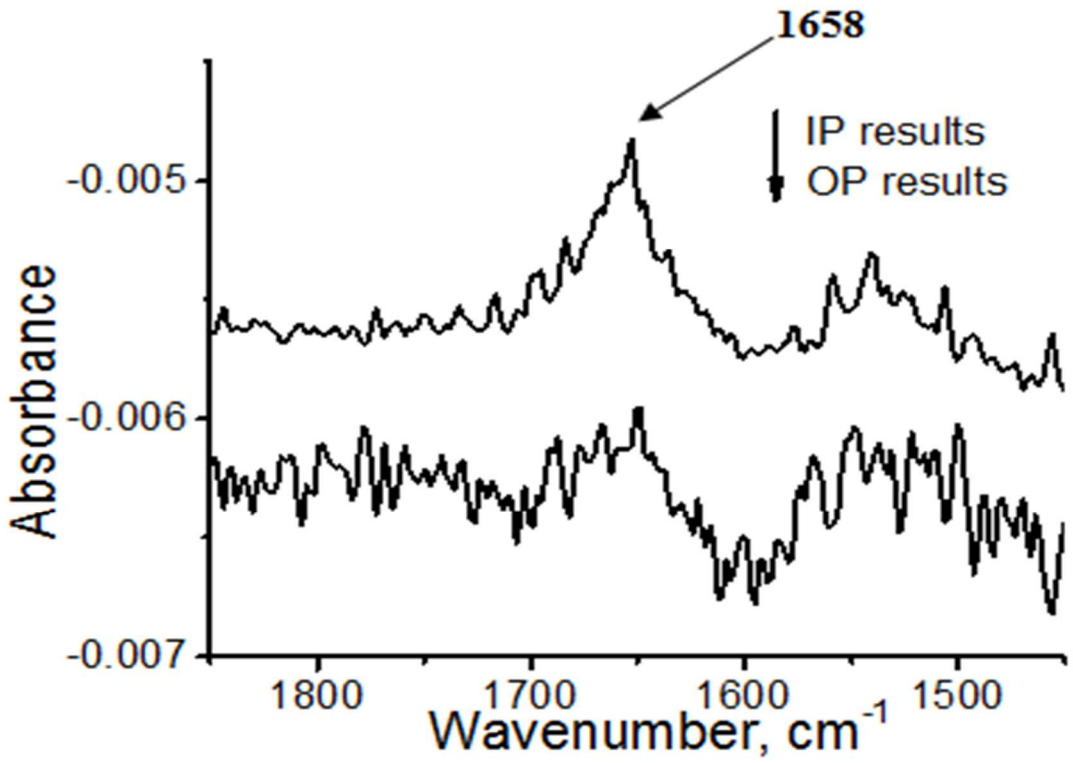


19. MAIRS spectra of α-synuclein (61-95) LB film on silicone slide.

# Chapter 4

## DISCUSSION AND FUTURE PERSPECTIVES

### 4.1 α-Synuclein (61-95) shows same properties to the whole protein of α-synuclein

The surface pressure-area isotherm of the α-synuclein (61-95) is found to form Langmuir monolayer as shown in Figure 16, which is similar to the whole protein of α-synuclein. Furthermore, the Langmuir monolayer of the α-synuclein (61-95) is also found to be stable at the air-water interface as shown in Figure 17 and 18, which is also similar to the whole protein of α-synuclein. α-Synuclein (61-95) is known to aid the development of Parkinson's disease, is found to show the same behavior to the whole protein of α-synuclein at the air-water interface, because the lipid-water interfacial layer is a region in the structure of lipid bilayer (see Section 1.4) responsible for the accumulation of α-synuclein in the presynaptic terminals.

### 4.2 Conformation change of α-synuclein (61-95) to α-helix

α-Synuclein (61-95) was also found to transform from an unstructured conformation in aqueous solution to α-helix at the interface as shown in Figure 18. This is responsible for the accumulation of α-synuclein (61-95) at the air-water interface. In addition, the air-water interface has been shown to have similar characteristics to the lipid-water interfacial layer (see Section 1.4), which is an example of cell membrane and vesicles. The nature of the lipid-water interfacial layer can also induce conformation change of α-synuclein (61-95). This conformation change may explain the stability of the Langmuir monolayer of α-synuclein (61-95).

### 4.3 Future perspectives

α-Synuclein (61-95) has been shown to form a stable Langmuir monolayer. The α-synuclein (61-95) Langmuir monolayer LB film of α-synuclein (61-95) has also been shown to adopt α-helix conformation in the LB film (see Figure 18) by CD and the molecular orientation has been studied and found to be parallel (see Figure 19) by MAIRS. However, the signal to noise ratio present in the MAIRS result is low, and there is also water vapor detected in the infrared spectra. Therefore, the sensitivity of MAIRS will be improved, in order to reduce the signal to noise ratio. Furthermore, the orientation of the whole protein of α-synuclein will be studied by MAIRS.

## REFERENCES

1. Fox, Micheal J. Parkinson's Diagnosis Questions. www.michaeljfox.org/living_aboutParkinsons parkinsons101.cfm.

2. National Institute of Neurological Disorders and Stroke, Parkinson's Disease Information Page. Dec 06, 2017.

3. Mark S. Forman, Virginia M-Y. Lee, Trojanowski Q, John Nosology of Parkinsons Disease: Looking for the Way Out of a Quackmire. Neuron. **2005**, 47 (4), 479.

4. Moore DJ1, West AB, Dawson VL, Dawson TM Molecular pathophysiology of Parkinson's disease. Annu. Rev. Neurosci. **2005**, (28), 57-87.

5. Dalfó, Esther, Evidence of Oxidative Stress in the Neocortex in Incidental Lewy Body Disease. Journal of Neuropathology & Experimental Neurology **2005**, 64 (9), 816-830.

6. Chinta, S. J. Andersen, J. k. Dopaminergic Neurons. The International Journal of Biochemistry & Cell biology. **2005**, (37), 942-946. 10.1016/j.biocel.2004.09.009.

7. Spillantini, M. G. Alpha-Synuclein in Filamentous Inclusions of Lewy bodies from Parkinson's disease and Dementia with Lewy bodies. Proc. Natl. Acad. Sci. U. S. A. **1998**, 95 (11), 6469-73.

8. Spillantini M.G, Schmidt M.L, Lee V.M, Trojanowski JQ, Jakes R, Goedert M. Alpha-synuclein in Lewy bodies. 1997.

9. Goderis, Lies. Interaction of Alpha-synuclein with Charged and Non Charged Surfactants. 2015.

10. Caughey, B., and Lansbury P. T. Protofibrils, Pores, Fibrils, and Neurodegeneration: Separating the Responsible Protein Aggregates from the Innocent Bystanders. Annu. Rev. Neurosci. **2003**, (26), 267-298.

11. Fink, A. L. The Aggregation and Fibrillation of Alpha-synuclein. Acc. Chem. Res. **2006**, 39 (9), 628-634.

12. Dusa, A. Characterization of Oligomers During Alpha-synuclein Aggregation Using Intrinsic Tryptophan Fluorescence. Biochemistry **2006**, 45 (8), 2752-2760.

13. Pfister, P.; Corti, N.; Hobbie, S.; Bruell, C.; Zarivach, R.; Yonath, A.; Bottger, E. C. 23S rRNA Base Pair 2057-2611 Determines Ketolide Susceptibility and Fitness Cost of the Macrolide Resistance Mutation 2058A -> G *Proc. Natl. Acad. Sci. U. S. A.* **2005**, *102*, 5180.

14. Proteins Structural Levels. In *Wordpress*, Biochemistry, Biomechanic April 2, **2013**.

15. Floudas, C. A.; Fung, H. K.; McAllister, S. R.; Monnigmann, M.; Rajgaria, R., Advances in Protein structure Prediction and Denovo Protein Design: A review. *Chem. Engin. Sci.* **2006**, *61*, 966-988.

16. Robinson, N. E.; Robinson, A. B., Review Article: Use of Merrifield Solid Phase Peptide Synthesis in Investigations of Biological Deamidation of Peptides and Proteins. *Biopolymers* **2008**, *90*, 297-306

17. Zhu, M., and Fink A. L., Lipid Binding Inhibits Alpha-synuclein Fibril Formation. J Biol. Chem. **2003**, 278 (19), 16873-16877.

18. Munishkina, L. A., Conformational Behavior and Aggregation of Alpha-synuclein in Organic Solvents: Modeling the Effects of Membranes. Biochemistry **2003**, 42 (9), 2720-2730.

19. Jeff Hardin, G. P. B., Lewis J. Kleinsmith, Becker's World of the Cell. *Department of Biology Memorial University of Newfoundland* 2012.

20. Ji, Xiaojun**.,** (CdSe) ZnS Quantum Dots and Organophosphorus Hydrolase Bioconjugate as Biosensors for Detection of Paraoxon. The Journal of Physical Chemistry B **2005**, 109 (9), 3793-3799.

21. Decatur, S. M., IR Spectroscopy of Isotope-Labeled Helical Peptides: Probing the Effect of N-acetylation on Helix Stability. Biopolymers **2000**, 54 (3), 180-185.

22. Cherepanov, Dmitry A., Low Dielectric Permittivity of Water at the Membrane Interface: Effect on the Energy Coupling Mechanism in Biological Membranes. Biophysical Journal **2003**, 85 (2), 1307-1316.

23. Wang, C, Alpha-synuclein in Alpha-helical Conformation at Air-water Interface: Implication of Conformation and Orientation Changes During its Accumulation/Aggregation. Chem. Commun. (Camb) **2010**, 46 (36), 6702-6704.

24. Jiang, Dianlu. A Kinetic Model for β-Amyloid Adsorption at the Air/Solution Interface and Its Implication to the β-Amyloid Aggregation Process. The Journal of Physical Chemistry B **2009**, 113 (10), 3160-3168.

25. Jiang, D. Redox Reactions of Copper Complexes Formed with Different Beta-amyloid Peptides and their Neuropathological (correction of Neuropathalogical) Relevance. Biochemistry **2007**, 46 (32), 9270-9282.

26. Wang,C.; Micic, M.; Ensor, M.; Daunert, S.; Leblanc, R.M. J. Cholesterol Mediates Chitosan Activity on Phospholipid Monolayers and Langmuir-Blodgett Films. J. Phys. Chem. B. **2008**, 112, 4146–4151.

27. Foggia, M.; Taddei, P.; Torreggiani, A.; Dettin, M.; Tinti, A. *Self-assembling Peptides for Biomedical Applications: IR and Raman Spectroscopies for the Study of Secondary Structure*. **2012**, Vol. 2, p 231-272.

28. Shioya, N., Norimoto, S., Izumi, N., Hada, M., Shimoaka, T., & Hasegawa, T. Optimal Experimental Condition of IR pMAIRS Calibrated by Using an Optically Isotropic Thin Film Exhibiting the Berreman Effect. *Applied Spectroscopy* **2017***, 71* (5), 901-910.

29. Belbachir, K. Orientation of Molecular Groups of fibers in Nonoriented Samples Determined by Polarized ATR-FTIR Spectroscopy. Anal. Bioanal. Chem. **2011**, 401 (10), 3263-3268.

30. A.J.Alder, N. J. G. a. G. D. F. Circular Dichroism and Optical Rotary Dispersion of Proteins and Polypeptides. *Meth. Enzymology 27*.

31. Treuel, L.; Malissek, M.; Gebauer, J. S.; Zellner, R. The influence of Surface Composition of Nanoparticles on their Interactions with Serum Albumin. *Chemphyschem: a European journal of chemical physics and physical chemistry* **2010**, *11* (14), 3093-3099.

32. Alrashdi, S. Synthesis, Purification, and Surface Chemistry of α-Synuclein (61-95). Ms. Thesis, Middle Tennessee State University June, 2018.

33. Oladimeji, S. O.; Saad A. A.; Hasegawa, T.; Wang, C.; Leblanc. R.M. J. NAC Part of α-Synuclein Also Transforms to α-Helix at the Interface with Parallel Orientation: Surface Chemistry and Spectroscopic Study of α-Synuclein (61-95). In preparation for submission 2019.